

Research Article

Bhre Wangsa Lenggana, Aditya Rio Prabowo*, Ubaidillah Ubaidillah, Fitriani Imaduddin, Eko Surojo, Haris Nubli, and Ristiyanto Adiputra

Effects of mechanical vibration on designed steel-based plate geometries: behavioral estimation subjected to applied material classes using finite-element method

<https://doi.org/10.1515/cls-2021-0021>

Received Feb 03, 2021; accepted Apr 29, 2021

Abstract: A research subject in structural engineering is the problem of vibration under a loading object. The two-dimensional (2D) model of a structure under loading is an example. In general, this case uses an object that is given a random frequency, which then causes various changes in shape depending on the frequency model. To determine the difference in performance by looking at the different forms of each mode, modal analysis with ANSYS was used. The samples to be simulated were metal plates with three variations of the model, namely, a virgin metal plate without any holes or stiffness, plates with given holes, and metal plates with stiffness on one side. The model was simulated with modal analysis, so that 20 natural frequencies were recorded. The sample also used different materials: low-carbon steel materials (AISI 304), marine materials (AISI 1090), and ice-class materials (AR 235). Several random-frequency models proved the deformation of different objects. Variations of sheet-metal designs were applied, such as pure sheet metal, giving holes to the sides, and stiffening the simulated metal sheet.

Keywords: modal analysis, random vibration, designed plate, steel class, finite-element method

1 Introduction

In recent years, structural engineering has become a popular topic of discussion. The problem of the vibration of a structure under loading or a moving force, which is included in the problem of moving loading, has become a research topic because vibration is a common case of moving-load problems, such as in railroads, overhead cranes, ballistic systems, magnetic discs, cable lines, building plates, and bridges. To achieve certain objectives, simulated two-dimensional modeling and efficient analytical methods are required for the reliable design and maintenance of a structure. In addition, this modeling and these methods can be used to accurately predict the vibration characteristics of structures. In general, structures under moving loads are modeled as one- (1D) or two-dimensional (2D) structures.

In this regard, several analytical methods were proposed for the vibration analysis of the problem of moving loads in one- and two-dimensional models. Some of them are the modal-analysis [1–4], integral-transformation (ITM) [5–7], Galerkin [8, 9], differential-quadrature [10, 11], finite-difference [12, 13], finite-element method (FEM) [14–18], dynamic-stiffness [19, 20], and frequency-domain spectral-element (SEM) [21–25] methods. The finite-element method (FEM) is a numerical procedure that can be applied to solve a wide variety of problems in engineering and science. In general, this method is used to solve steady, transient, and linear and nonlinear problems in electromagnetic fields, structural analysis, and fluid dynamics [1]. The finite-element method has the main advantage of being able to handle all kinds of geometries and nonhomogeneous materials without the need to change computer-code formulations. The idea of this method is to break the problem into a large number of planes, each with a simple geometry, to facilitate problem solving. As a result, the domain breaks down into a number of small elements, and the problem goes from small but difficult to solve to large and relatively

***Corresponding Author: Aditya Rio Prabowo:** Department of Mechanical Engineering, Universitas Sebelas Maret, Surakarta, Indonesia; Email: aditya@ft.uns.ac.id

Bhre Wangsa Lenggana, Ubaidillah Ubaidillah, Fitriani Imaduddin, Eko Surojo: Department of Mechanical Engineering, Universitas Sebelas Maret, Surakarta, Indonesia

Haris Nubli: Interdisciplinary Program of Marine Convergence Design, Pukyong National University, Busan, South Korea

Ristiyanto Adiputra: Department of Marine Systems Engineering, Kyushu University, Fukuoka, Japan

easy to solve. Through the process of discretization, linear algebra problems are formed with many unknowns. In an electromagnetic case, a discretization scheme, as implied by FEM, which implicitly combines most of the theoretical features of the analyzed problem, is the best solution for obtaining accurate results in problems with complex, nonlinear geometries [2, 3]. This method can also be used for complex differential equations that are very difficult to solve.

To investigate the vibrational characteristics of complex structures subjected to moving loads, FEM is extensively used. The shape function used in FEM is independent of the vibration frequency of a structure. FEM generally requires the very fine discretization of structures to obtain reliable solutions, especially in the high-frequency range [26–28]. This paper analyzes a series of designed plate geometries that are set as representative of structural components. Several steel classes are applied to the plates in a finite-element simulation as consideration of various structural types, *e.g.*, marine and offshore structures, and inland infrastructure. Vibrational analysis is the focus of the current work, which is directed to quantify the natural frequency characteristics of the designed plates.

2 Literature review

2.1 Introduction to finite-element method

The finite-element method (FEM) is process analysis carried out by dividing a certain quantity into smaller pieces to obtain a large-class engineering analysis solution. Mathematically, FEM is an approximate approach that serves to solve field problems. The finite-element method is also commonly referred to as finite-element analysis (FEA) [16, 23]. One of the reasons for using FEA is because it is a powerful computational technique used to solve various engineering problems, especially those with complex geometries that are subject to general boundary conditions. Analysis was carried out with field variables that varied from point to point. Thus, this analysis has an infinite number of solutions in the domain [23]. This makes the problem need fairly complex analysis. For that reason, using FEA is necessary. In reality, the system comprises a number of parts – expression elements – that are not known in terms of the assumed function estimates in each element. For each element, a variational or weighted residual method is applied to create a systematic approximate solution [26]. These functions are usually called interpolation functions, and are then entered in terms of field variables at certain points, called nodes.

The nodes that are formed are connected to the connected elements and are usually located along the boundary of the element. This method is used as an analytical tool to solve engineering problems because the degree of flexibility in distinguishing irregular domains from finite elements. In general, the use of FEA is carried out to create new product designs and improve the development of existing products. This makes FEA popular for researchers to verify proposed designs prior to a prototyping or construction process. The goal is to find out the feasibility of a design produced for an application. FEA is very widely used in the structural field [15]. Structural analysis consists of linear and nonlinear models. The linear model considers simple parameters and assumes that the material does not undergo plastic deformation, while the nonlinear model assumes that the structure undergoes plastic deformation as a result of the initial load. In general, FEA uses three types of analysis, namely, 1D modeling to solve beam, rod, and frame elements; 2D modeling, which is useful for solving field-stress and plane-strain problems; and 3D modeling, which is useful for solving complex solid structures.

2.2 Implementation of FE calculation

Several years earlier, solutions for plate deflection under different boundary conditions were proposed by several researchers. Bhattacharya investigated plate deflection under static and dynamic loading using new finite-difference analysis. The actual mode shape of the plates of each node was found in this study, and this approach provides a fourth-order biharmonic equation that varies from node to node [29]. A mathematical approach to the large deflection of rectangular plates was also presented by Defu and Sheikh [30], who analyzed on the basis of second-degree and fourth-order Von Karman partial differential equations. In their research, lateral deflection with respect to the applied load was found, which made this solution usable in the direct practical analysis of plates under different boundary conditions [30]. In the same field, Bakker *et al.* studied a forecast analysis method for large deflections of rectangular thin plates with simple supported boundary conditions under the action of transverse loads. This approach was taken to find initial deflection shape and the total plate. From this analysis, the deflection behavior of the plate size under transverse load can be expressed as a function of the plane stiffness of the plate before buckling [31]. Furthermore, research was carried out by Liew *et al.*, who developed the differential quadrature method and the harmonic differential quadrature method for the static analysis of three-dimensional rectangular plates. A

study conducted by Liew *et al.* aimed to find the bending and bending of plates that were supported and clamped only at boundary conditions [32].

In the utilization of FEA, some researchers made use of it in solving the perforated-plate problem. Jain analyzed the effect of the ratio of a perforated plate D/A (D is hole diameter, and A is plate width) on the stress concentration and deflection factors in isotropic and orthotropic plates under transverse static loading [33]. The point put forward by Jain (2009) was related to and supported by research by Chaudhuri (1987), who presented the theory of stress analysis using the rhombic array of alternating method for several circular holes [34–36]. In that study, the effect of stress concentration on perforated laminated plates using the finite-element method was investigated. Then, Paul and Rao presented a theory for the evaluation of stress concentration factors for thick laminated plate and fiber-reinforced plastic (FRP) with the help of the Lo-Christensen-Wu high-order bending theory under transverse loading [37].

Furthermore, in the last few decades, authors developed examining plates with stiffeners. Although rigid rectangular plates are thoroughly studied, the application of stiffeners to round plates is not very popular. The deflection in isotropic coiled plates subjected to two stiffening rings under static pressure was studied by Steen and Byklum. The used methodology was with clamped boundary conditions during analysis. Previously, Troipsky worked on rigid plates under bending, stability, and vibration. Pape and Fox presented an infinite series approach to the correctness of the plate aspect ratio using a rigid elastic beam [36–38].

Further development was carried out by Xuan *et al.*, who performed element refinement using the boundary integral method. Das *et al.* developed a fairly general classical method that could be applied to all boundary conditions. Meanwhile, Jain in his research presented analysis of stress concentrations and deflections on isotropic and orthotropic rectangular plates with circular holes under transverse statistical loading. His research assessed three types of elements to solve the problem of square triggers with various boundary and load conditions [33, 39, 40].

The plasticity characteristics and external lateral loading of an elastoplastic plate were developed by Moshaiov and Vorus using an integral equation formulation for bending an elastoplastic plate. Formulations for Kirchhoff plate analysis with subregions by varying thickness for the boundary element method were also developed by researchers such as Paiva and Aliabadi. The development can be used to analyze the floor of a building in such a way that the integral equation of the curvature boundary of the points located at the zone interface is inferred very easily, which allows for the bending moment to be ob-

tained [41, 42]. FEM is a numerical or computational technique that can be used to solve different field variables such as displacement, stress, strain, temperature, and electric charge that have certain boundary conditions [43, 44]. The application of the finite-element method is exemplified simply in Figure 1, where the physical (real) system is assumed by a mathematical model, and the discretization of FEA was applied to it. After a good representation of the real physical system into the mathematical model, and increased discretization, the FEM solution approaches the exact solution to the mathematical model, called convergence in FEM analysis. Hence, when used effectively, FEM can enable innovations that are not possible.

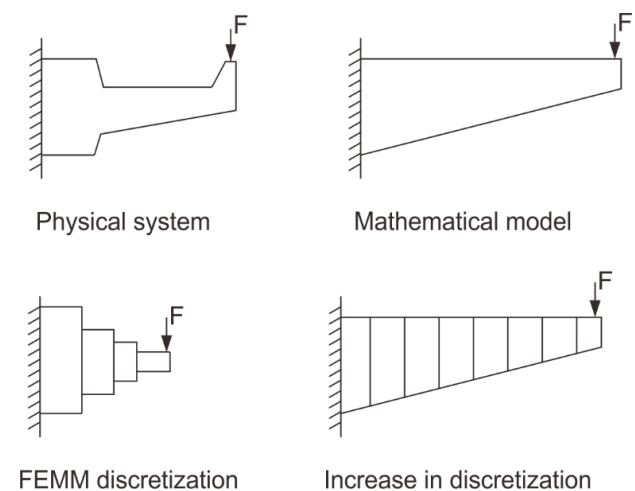


Figure 1: Approximate nature of finite-element analysis (FEA)

Different static and dynamic engineering problems can be solved using the finite-element method, ranging from simple beam structural-stress analysis (1D) or complex machines with very large capacities (3D), to dynamic responses under mechanical, electrical, magnetic, or thermal differences. The use of the finite-element method is very widespread in various industrial fields, such as the aerospace, aeronautical, defense, consumer-product, and industrial-equipment industries. In addition, with the rapid development of different computer-aided design (CAD) software and advanced computing systems, the application of FEM has penetrated into materials science, biomedical engineering, medicine, biology, and physics [22]. Table 1 summarizes some examples of applications using FEM.

Table 2 provides different FEM application disciplines with degrees of freedom (DOF) and loading vectors. In this table, DOF is an unknown parameter that must be solved using Equation (1) which is the global displacement matrix [23].

Table 1: Finite-element method (FEM) applications [22]

Field	Application examples
Solid/structural mechanics	Wind-turbine blade design optimization, structure-failure analysis, crash simulation, nuclear-reactor component integrity analysis, beam and truss design and optimization, limit-load analysis
Heat conduction	Combustion engine, cooling and casting modelling, electronic cooling modelling
Acoustic flow	Seepage analysis, aerodynamic analysis of cars and airplanes, air-conditioning modelling of buildings
Electronics/electromagnetics	Electromagnetic-interference suppression analysis, sensor and actuator field calculations, antenna-design performance predictions

Table 2: Degrees of freedom (DOF) and loading vectors for different disciplines using FEM

Discipline	DOF (U)	Loading vector (R)
Solid-structure mechanics	Displacement	Force
Electrostatic	Electropotential	Charge density
Heat conduction	Temperature	Heat flux
Computational fluid dynamics (CFD)	Displacement potential, pressure, velocity	Particle velocity, fluxes
Magnetostatic	Magnetic potential	Magnetic intensity

In general, the value of stiffness and mass on a structural plate is known in the form of a matrix. Stiffness and mass matrices are denoted by $[K]$ and $[M]$, respectively; then, the equation of motion of the system can be expressed as in Equation (1).

$$[M] \{\ddot{\mathbf{u}}\} + [K] \{\mathbf{u}\} = \{0\}, \quad (1)$$

where $\{\ddot{\mathbf{u}}\}$ and $\{\mathbf{u}\}$ are the acceleration and displacement vectors, respectively, so that in free vibration, the values of the acceleration and displacement vectors can be formulated according to Equations (2) and (3) as follows [24].

$$\{\mathbf{u}\} = \{\bar{\mathbf{u}}\} e^{\bar{i}\omega t} \quad (2)$$

$$\{\ddot{\mathbf{u}}\} = -\bar{\omega}^2 \{\bar{\mathbf{u}}\} e^{\bar{i}\omega t}, \quad (3)$$

where $\{\bar{\mathbf{u}}\}$ is the amplitude of the vector $\{\mathbf{u}\}$; thus, Equation (1) can be substituted into Equation (4) as follows [24].

$$([K] - \bar{\omega}^2 [M]) \{\bar{\mathbf{u}}\} = \{0\} \quad (4)$$

To obtain the characteristic equation of an attached structural plate, Equation (5) is used [24].

$$|[K] - \bar{\omega}^2 [M]| = 0. \quad (5)$$

FEM is most widely used in linear and nonlinear static analyses. The various types of static problems that the FEM solves in this area include the analysis of elastic, elastoplastic, and viscoplastic beams, frames, plates, shells, and solid

structures. Typically, static analysis includes the analysis of stress, strain, and displacement under static loading for one-, two-, or three-dimensional problems. In this chapter, the general theory of elasticity is discussed. In addition, the general formulation of the stiffness of 1D, 2D, and 3D elements is discussed with the detailed formulation of the stiffness matrix of the beam elements. After that, general solution methods of static analysis are shown for linear and nonlinear problems. The global equation for static analysis is the same as that in Equation (1), and solving for the static problem is exactly the same as the one mentioned above in the general FEM procedure.

The main objective of any stress analysis is to find the distribution of displacement and stress under static loading and limit conditions. The following equations are fulfilled if there is an analytical solution to a particular problem based on elasticity theory. Table 3 shows the types of equations in 1D, 2D, and 3D problems.

Problems that exist in real life are often solved by taking a mathematical approach. In addition to a mathematical approach, either experimenting by producing a prototype model with a certain scale or the original is also a solution to finding the solution to a problem. Mathematical modeling is a process of interpreting existing problems with the aim of simplifying and accelerating problem solving. This makes mathematical modeling both challenging and demanding, as the use of mathematics and computers to solve real-world problems is extensive and affects all branches of learning.

Table 3: Type and number of equations in 1D, 2D, and 3D problems [25]

Types of equation	Number of equations		
	3D problems	2D problems	1D problems
Equilibrium equation	3	2	1
Stress-displacement relation	6	3	1
Strain-stress relation	6	3	1
Total no. of equations	15	8	1

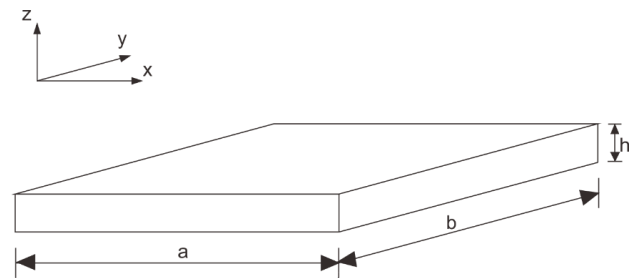
Problem solving with a mathematical modeling approach is possible with software. A powerful finite-element piece of software for analyzing different problems is ANSYS. Various problems can be overcome with ANSYS such as elasticity, fluid flow, heat transfer, and electromagnetism. Nonlinear and transient analyses can also be completed with the software. In general, ANSYS analysis has the following steps for problem solving: First, modeling, a process that includes the definition of system geometry and the selection of material properties. In this step, the user can draw a 2D or 3D representation of the problem. Second, meshing. This step involves discretizing the model according to predefined geometric elements [22–24]. This is followed by the retrieval of the result and solution, and this step involves applying boundary and load conditions to the system, and resolving problems. Lastly, post-processing, which involves plotting the nodal solution (unknown parameter), which may be displacement, stress, or reactive force.

2.3 Modal analysis and random vibration

The natural or resonant frequency is a fundamental resonance mode of a vibrating system. The natural frequency can also be defined as the frequency that vibrates when under a small impact load for a certain period of time. Important parameters that can represent the dynamic response of a test object in a vibration test are the natural frequency and mode shape of the object. To identify a dynamic characteristic such as natural frequency, the shape of the mode can be established using modal analysis [45, 46]. Modal analysis is based on the fact that the vibrational response of a linear time variant dynamic system can be expressed as a linear combination of a series of simple harmonic motions called natural vibration mode. The natural mode of vibration is generally determined entirely by its physical properties such as mass, strength, damping, and spatial distribution; this is also because the natural mode of vibration is inherent in dynamic systems [47–50]. Modal analysis is often used to abstract the modal parameters of a system, including natural frequency, mode shape, and modal damping

ratio. This parameter depends only on the system itself, but dominates the system response to excitation. Modal analysis is the fundamental response of analysis and is of increasing concern. Experimental modal analysis (EMA) can estimate the natural frequency, mode shape, and damping value of a measured structure [51]. The finite-element (FE) model structure can be validated by comparing the experimental natural frequency and mode shape with the results of FE model analysis. Modal analysis is a technology of linear analysis that is used to determine the natural-frequency structure and vibration modes. In modal analysis, the only effective load is the zero-displacement limit. If a certain degree of freedom (DOF) determines a nonzero displacement limit, the program replaces the degrees of freedom with a zero displacement limit [52, 53].

Modal analysis is based on several basic equations with an overview of geometric problems, as shown in Figure 2 below, where E is Young's modulus, ρ is the density of the

**Figure 2:** Thin plate sketch geometry

material, and ν is Poisson's ratio. The plate geometry image has infinite degrees of freedom due to the determination of the location of each particle on the plate body, which has unlimited coordinates. In this case, deflection and linearity are assumed to be small values, so the equation for the bending motion of the plates can be found through Equation (6) below [54].

$$D\nabla^4 w + \rho h \frac{\partial^2 w}{\partial t^2} = 0 \quad (6)$$

$$\nabla^4 = \nabla^2 \nabla^2 \quad (7)$$

$$D = \frac{Eh^3}{12(1-\nu^2)}, \quad (8)$$

where w is the transverse deflection, ∇^2 is Laplacian, and Equation (8) is the plate flexural rigidity. Deflection is a function of x and y spatial coordinates, and from time function t . If the equation of motion is filled with form deflection functions, then the equation of motion can be written as follows.

$$w(x, y, t) = \varnothing(x, y) q(t), \quad (9)$$

where $\varnothing(x, y)$ is a function satisfying the plate boundary conditions, and $q(t)$ is the corresponding general coordinate. By adding the equations of motion and separating the variables, Equations (10) and (11) can be obtained [54].

$$\nabla^4 \varnothing - \frac{\omega^2}{D} \varnothing = 0 \quad (10)$$

$$\frac{d^2 q}{dt^2} + \frac{\omega^2}{\rho h} q = 0 \quad (11)$$

where ω is the natural frequency. The solutions of Equations (10) and (11) are solutions to infinite sets of eigenvalues and functions (or eigenvectors). In this case, the boundary conditions determine the natural frequency, and the initial conditions determine the contribution of each mode according to the vibration of the plate. To determine the natural frequency, several methods can generally be used, such as the Rayleigh, Rayleigh-Ritz, and FEM methods, shown in Equations (12), (14), and (15), respectively [54].

$$\omega^2 = \frac{V_{max}}{\frac{1}{2} h \rho \iint \varnothing(x, y) dx dy} \quad (12)$$

$$V_{max} = \frac{1}{2} \rho h \omega^2 \iint \varnothing^2(x, y) dx dy \quad (13)$$

$$\omega_n = \frac{\lambda_n}{a^2} \sqrt{\frac{D}{\rho h}}, \quad (14)$$

where V_{max} is the maximal velocity that can be formulated according to Equation (13), a is an unknown constant, and λ_n is the frequency parameter. In Equation (14), Rayleigh-Ritz, the natural frequency is written in the form of ω_n [54].

$$f = \frac{\omega}{2\pi}, \quad (15)$$

where ω is the natural circular frequency and f is the natural frequency. In Equation (15) of the FEM method, the equation of motion for the structure is formulated according to Equations (1–5).

Random-vibration analysis is used to determine the response of the structure under random loading. ANSYS

uses the power spectral density (PSD) spectrum as analysis of random vibrations from the load input. Power spectral density is a probability statistical method and the root-mean-square value of a random variable, including the measurement of random-vibration energy and frequency information. The power spectrum can be in the form of displacement, velocity, acceleration or power spectral density, and in other forms [55–59].

2.4 Pioneer works in FEM and structural vibration

FEM was first developed through advances in aircraft-structure analysis. The development of the FEM foundation was first carried out by Courant in the 1940s. In 1956, the stiffness matrix for frames, beams, and other elements was developed by Courant and others [60–64]. In the 1960s, the term “finite element” was first coined and used by Clough; later, Zienkiewicz and Chung published the first book on FEM in 1967. Computer FEM codes appeared during the 1970s, and to this day, advanced FEM codes are available for solving various field problems [65–70]. In the last few decades, FEM has shown very significant developments, especially in FEM software, including the introduction of p elements, integration sensitivity, FEM code on desktop computers, and the development of robust CAD programs for modeling complex geometries. A history of FEM is summarized in Table 4 [22].

Table 4: Type and number of equations in 1D, 2D, and 3D problems

Year	Major milestone
1943	Variation method which laid foundation of FEM (Courant)
1956	Stiffness method for beams, trusses
1960	Term “finite element” coined
1967	First book of FEM by Zienkiewicz and Chung
1970	FEM applied to nonlinear problems and large deformations
1970s	Computer implementation on solving FEM
1980s	Used in microcomputers and GUIs
1990s	Large structural system analysis, nonlinear and dynamic problems
2000s	Multiphysics and multiscale problems
2014s	Powerful FEA tools

3 Materials and methods

3.1 Setting and configuration for finite-element analysis

3.1.1 Design sketch

The sheet-metal scheme used in this study is shown in Figure 3. Figure 3a shows a metal-sheet scheme without stiffener or holes, Figure 3b is a metal sheet with holes, and Figure 3c is a metal sheet with a given stiffener. This was performed to determine the effect of having a stiffener and holes in the metal sheet with the same material. In this case, piercing a hole into the metal sheet obviously makes it the lightest material compared to the others, while the metal sheet with two stiffeners in a cross-sectional manner is the heaviest material. However, as Figure 3 shows, stiffener application was carried out with very small dimensions, so that the weight difference between the three material variations was not too far apart.

The three variations of the design sketch were simulated to determine which metal sheet was more effective from various perspectives, such as material weight, performance, and level of difficulty in manufacturing. The performance of each metal sheet was examined using finite-element analysis, which was randomly assigned a frequency.

3.1.2 Materials

The material to be used was one type of low-carbon steel material (AISI 304), marine material (AISI 1090), and ice class material (AR 235). Each type of material was simulated in the same way to examine the difference in results against a given random frequency. Table 5 shows the properties of each material. The properties of each material were then set in the ANSYS software according to the material data sheet.

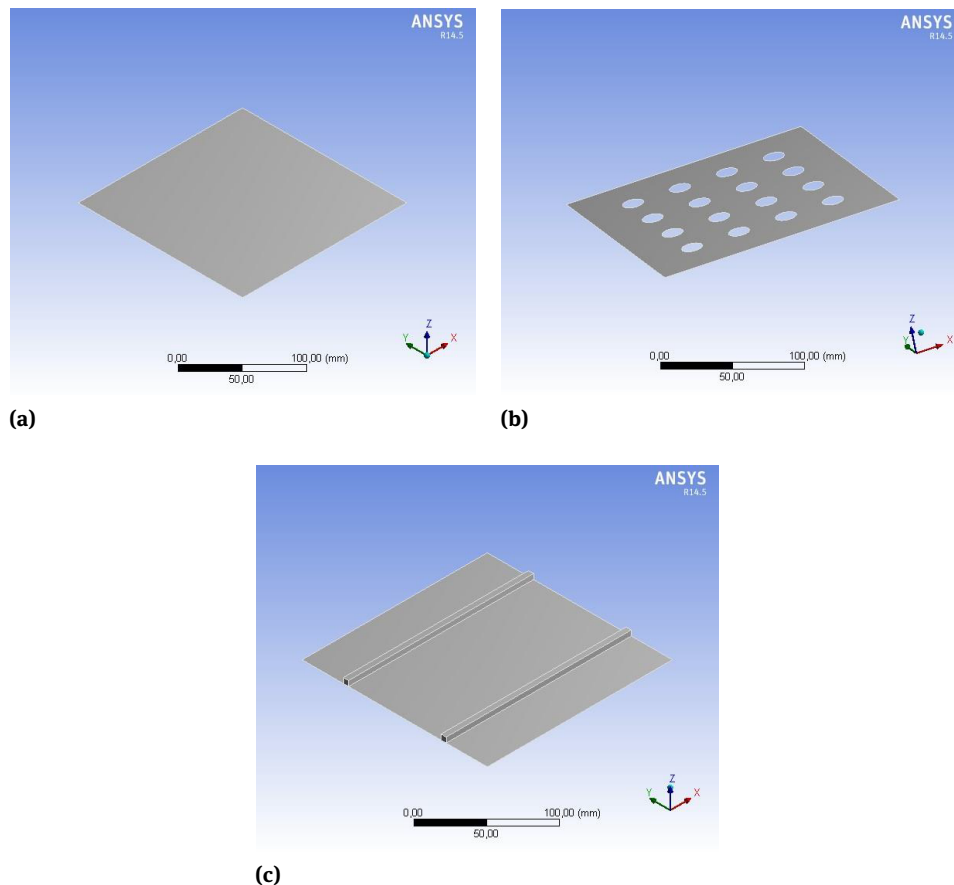


Figure 3: Design sketch model simulation of metal sheet: (a) virgin metal sheet; (b) hole metal sheet; (c) stiffener metal sheet

Table 5: Material properties of low-carbon steel AISI 304, AR 235, and AISI 1090 carbon steel

Properties	Ice-class material	Marine class material	Low-carbon steel	Unit
Tensile strength, ultimate	792	696	505	MPa
Tensile strength, yield	482.63	540	215	MPa
Modulus elasticity	210	210	200	GPa
Poisson's ratio	0.3	0.3	0.29	-
Shear modulus	80	80	80	GPa
Density	7.8	7.8	8	g/cc

3.1.2.1 Low-carbon steel

Carbon steel is a type of alloy steel consisting of iron (Fe) and carbon (C) elements, where iron is the basic element and carbon is the main alloying element. In the steel-making process, the addition of other chemical elements, such as sulfur (S), phosphorus (P), silicon (Si), manganese (Mn), and other chemical elements is in accordance with the desired properties of the steel. Low-carbon steel is steel with carbon-element content in a steel structure of less than 0.3% C. This low-carbon steel has high toughness and ductility, but low hardness and wear resistance. In general, this type of steel is used as raw material for the manufacture of building structural components, building pipes, bridges, car bodies, and others.

3.1.2.2 Marine materials

Marine materials generally use high-strength low-alloy steel materials. In this case, the material used is a type of HSLA steel material, namely, AR 235 Abrasion Resisting Steel. Abrasion Resisting Steel AR 235 is medium carbon and high manganese. This type of steel is tough and is wear-resistance ductile enough to allow for specific machining. The chemical composition of this type of steel gives a Brinell hardness of about 235 under as-roll conditions and tensile strength of about 115,000 psi. Abrasion-resistant steel has 2 to 10 times the service life of mild steel when used in scraper blades, mixers, manure-moving equipment, loaders, conveyors, scoop gear, pull-conveyor bottoms, spouts, shovels, mine screens, troughs, hoppers, truck body dumps, concrete buckets, fan blades, ore jumps, tail sluices, bucket lips, rock screens, loading channels, agitator oars, dredge pump liners, grinding pans, liner plates, and sluice gates. This steel, if not too cold, takes a 90° bend to a reasonable radius with a thickness of up to about 3/8 inches without any fracture by being gently bent (in degrees) until forming is complete. For more difficult forming and all heavier gauge forming, the gauge must be heated and shaped while hot. Heat forming should take place at an ambient temperature of 1500°F. If the steel is allowed to cool slowly, its abrasive

resistance qualities are not lost, nor are there any cracks or distortion. High-carbon steels such as this grade should not be worked by any method when it is very cold. This grade, due to its high hardness and toughness, is rather difficult for machines to work with. However, ordinary high-speed tools are more than capable of machining when needed.

3.1.2.3 Ice-class materials

Ice-class material is generally applied in the shipping sector, and is also known as polar-class material. This material is usually used for ship hulls with certain requirements. The layered structure is a rigid plate element that is in contact with the hull of the ship and is subject to ice loads. This requirement applies to an inboard level that is lower than the height of the adjacent truss or parallel supports, or 2.5 times the depth of the frame cutting the layered structure. The thickness of the lining and the slightest amount of installed stiffening is such that the level of attachment of the required ends for the shell frame must be ascertained. Class associations have various rules covering requirements and qualifications on ships intended to operate in icy waters, a set of rules made up of several ice notations. Meanwhile, notation generally depends on the geographic area of operation, and differs with respect to operational capability and structural strength. Depending on the ship's destination and area of operation, the owner is responsible for selecting the appropriate ice-class notation on the ship. Initially, the elastic approach and structural capacity definition put forward by the Finnish–Swedish Ice Class Rules (FSICR) regarding ships were used to ensure safe operations in the Baltic Sea during winter. In this case, prescribed notations are those used to determine the minimal requirements for engine power and ice reinforcement for the ship, assuming that icebreaker assistance is available when needed. Initially the regulations were aimed at operating merchant ships crossing ice routes. All polar-class vessels require effective protection against abrasion caused by ice and against corrosion. The most important part of this protection is applied to all surface coatings of polar-class ships. Polar-class ves-

sels have a minimal corrosion/abrasion addition $t_c = 1.0$ mm applied to all internal structures within the hull area reinforced by ice, including layered members adjacent to shells, and rigid nets and flanges.

3.1.3 Geometry and boundary condition

Three different sheet-metal designs with the same material were simulated against a given random vibration. Further-

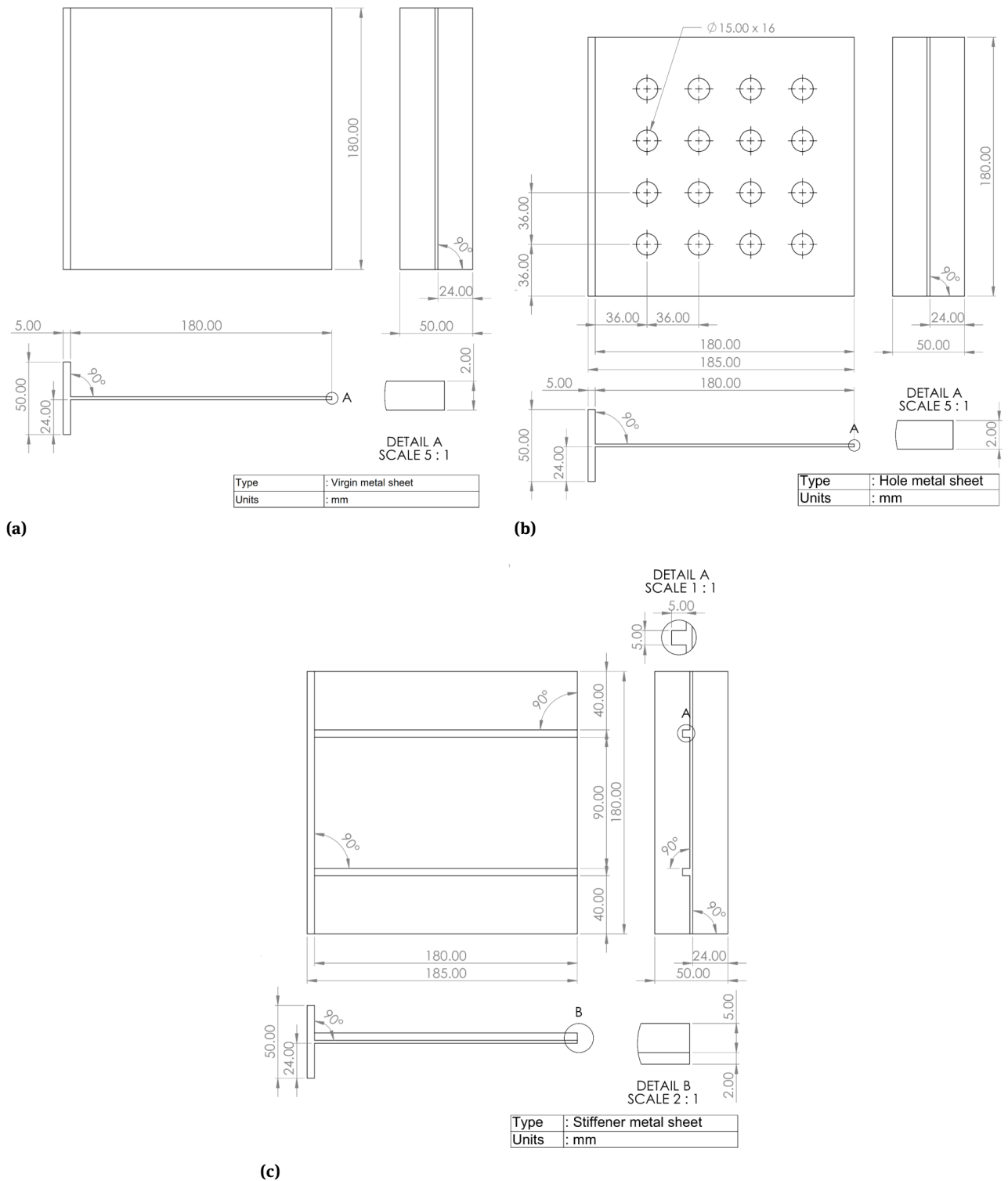


Figure 4: Technical drawing of models and sketch application: (a) virgin metal sheet; (b) hole metal sheet; (c) stiffener metal sheet

more, 20 modes of total deformation for each sheet were seen in value, but not all forms of the total deformation were shown. Two form modes of total deformation were shown. This mode was taken because it represents a change in the shape of each design. Each metal-sheet design had the same main dimensions of 180 × 180 mm. The first design was a metal sheet without any variation in either holes or

stiffener, the second design was a perforated metal sheet with 16 holes and a diameter of 15 mm in each hole, and the third design was a sheet metal with two stiffeners as shown in Figure 3a–c with a thickness of 2 mm.

The total deformation of each metal sheet was obtained through modal analysis simulation in ANSYS. In addition to using modal analysis, a harmonic-response simulation

Table 6: Natural frequencies of low-carbon steel material on different models

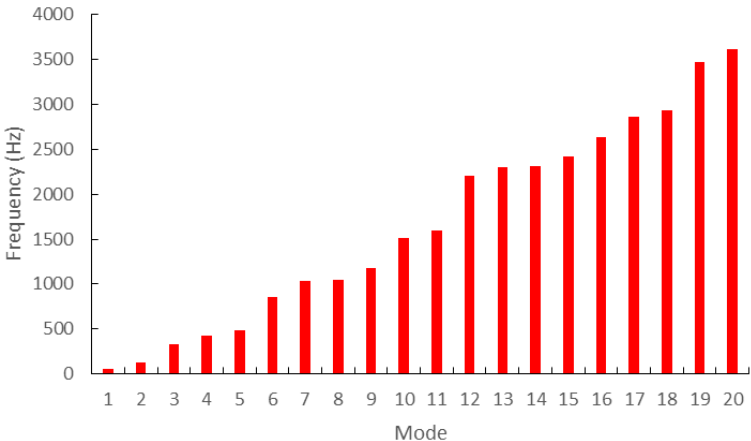
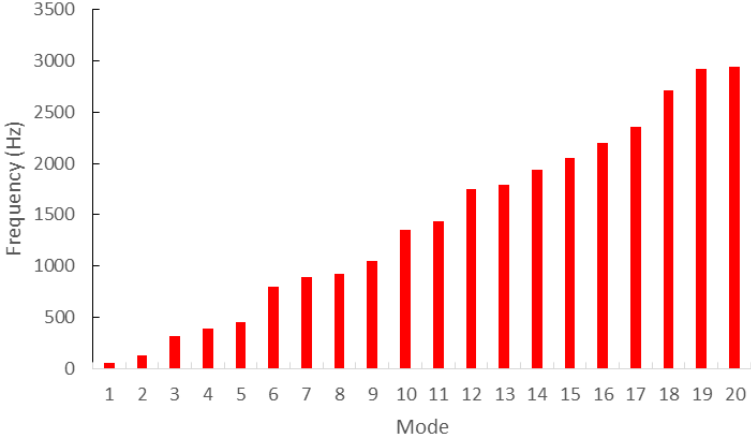
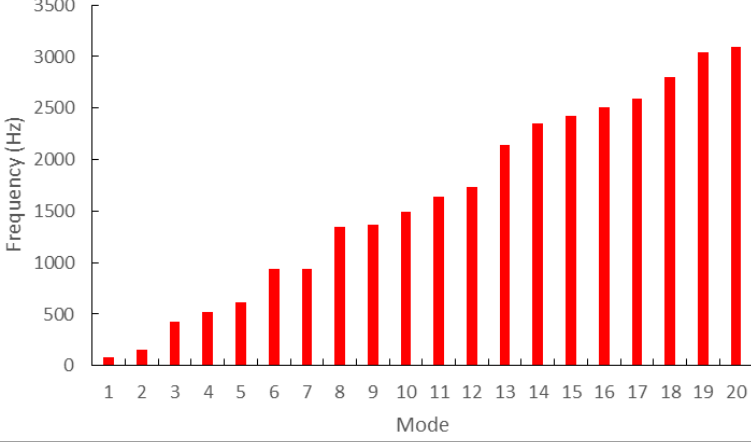
Variant	Result
Virgin metal sheet	
Hole metal sheet	
Stiffener metal sheet	

Table 7: Natural frequencies of low-carbon steel, marine, and ice-class materials on different models

Mode	Natural frequency (Hz)								
	Virgin			Hole			Stiffener		
	Low	Marine	Ice class	Low	Marine	Ice class	Low	Marine	Ice class
1	52.509	54.447	54.621	50.57	52.401	52.569	82.028	84.944	85.215
2	129.56	133.76	134.19	125.05	129.11	129.53	152.45	157.4	157.9
3	333.29	344.95	346.06	312.71	323.67	324.7	430.23	444.99	446.41
4	420.55	435.9	437.29	386.65	400.32	401.6	520.29	538.81	540.54
5	483.05	499.41	501.01	457.41	472.89	474.4	617.91	638.57	640.62
6	850.48	879.29	882.1	793.07	819.82	822.44	936.88	969.41	972.51
7	1032.0	1070.5	1073.9	895.41	927.99	930.95	938.04	971.15	974.26
8	1048.7	1085.7	1089.2	923.18	955.67	958.73	1351.5	1398.8	1403.3
9	1181.3	1224.5	1228.4	1046.3	1083.4	1086.9	1369.5	1416.3	1420.8
10	1508.9	1562.1	1567.1	1354.5	1401.4	1405.9	1497.9	1549.5	1554.4
11	1596.7	1652.0	1657.3	1435.0	1484.6	1489.3	1641.0	1697.3	1702.7
12	2201.5	2281.2	2288.5	1751.4	1814.1	1819.9	1732.7	1797.0	1802.7
13	2297.2	2384.1	2391.7	1795.9	1861.3	1867.3	2139.0	2215.9	2223.0
14	2309.8	2389.7	2397.4	1932.9	2001.9	2008.3	2355.5	2437.2	2445.0
15	2420.1	2508.8	2516.9	2056.4	2127.8	2134.7	2424.7	2510.5	2518.5
16	2635.0	2729.8	2738.5	2199.5	2276.8	2284.1	2503.1	2588.9	2597.2
17	2857.3	2960.5	2970.0	2356.5	2439.7	2447.6	2592.7	2684.7	2693.3
18	2933.2	3030.2	3039.9	2713.4	2803.6	2812.5	2798.5	2890.9	2900.1
19	3476.4	3599.1	3610.6	2922.1	3025.3	3035.0	3042.1	3154.8	3164.9
20	3613.5	3739.7	3751.7	2940.1	3045.2	3055.0	3089.1	3198.2	3208.4

model was also established in ANSYS to obtain the frequency value for the amplitude of the metal sheet. In performing the harmonic-response simulation process, one side of the metal sheet was set as the fixed mode, and the sheet metal was given a constant force of 300 N. Figure 4a shows the dimensions of the design sketch used in the simulation, while Figure 4b is a design application model represented by a design scheme.

4 Results and discussion

The natural frequency of each sheet-metal design was obtained through modal analysis in ANSYS. Natural frequencies are shown in Tables 6 and 7, which are graphs and values in Hz. There were differences in the natural-frequency values of each sheet-metal design. Some examples are natural frequencies in Modes 3 and 12 for sheet metals. In Mode 3, the sheet metal without holes and a stiffener had a natural-frequency value of 333.29 Hz, the sheet metal with holes had a natural-frequency value of 312.71 Hz, while the sheet metal with a stiffener had a natural-frequency value of 430.23 Hz. The sheet metal with stiffener application had

the largest natural-frequency value in Mode 3. However, in Mode 12, the largest natural-frequency value was achieved by the sheet-metal design without holes and stiffener, and the natural-frequency value for the sheet metal with a stiffener was even smaller than the natural-frequency value of the sheet metal with holes.

The natural-frequency value for the sheet metal without holes and stiffener reached 2201.5 Hz, the natural-frequency value for the sheet metal with holes was 1751.4 Hz, and the sheet metal with a stiffener had the lowest value of 1732.7 Hz because Modes 3 and 12 had different deformations, which Table 8 shows. Table 8 also shows the contours of pressure distribution and shape that occurred in Modes 3 and 12 for each design.

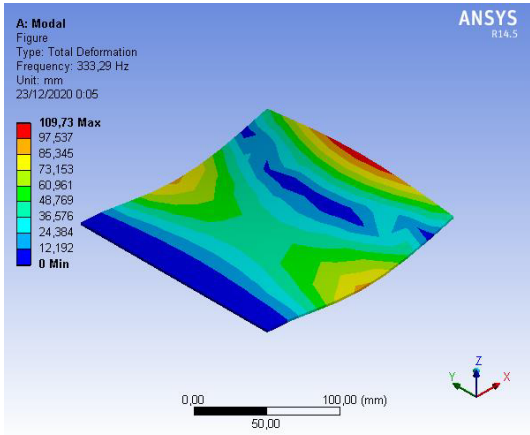
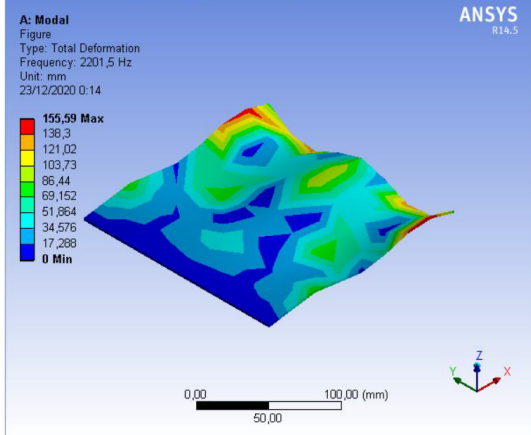
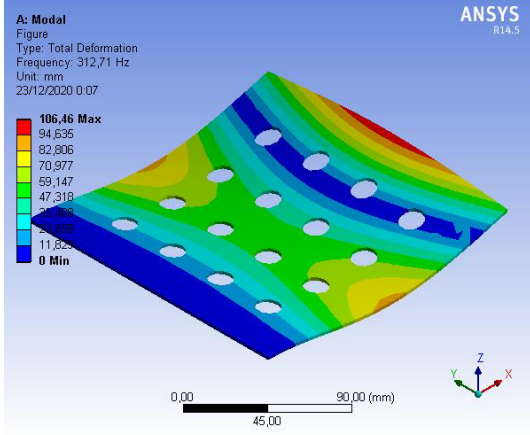
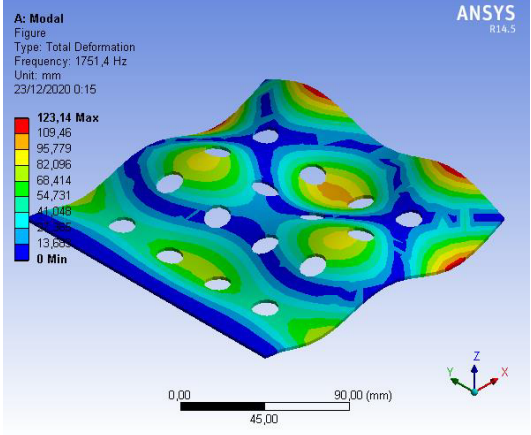
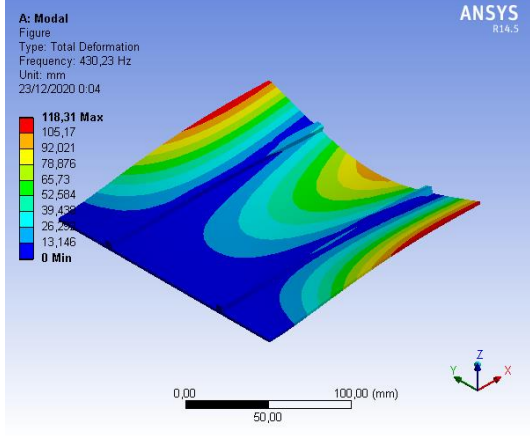
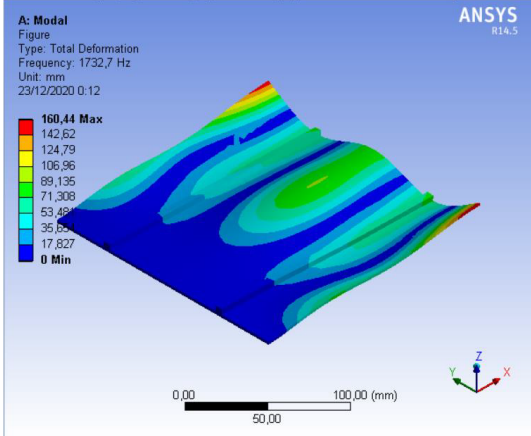
Figure 4 shows a graph of the frequency and amplitude that occurred in all the models with the same material: (a) virgin metal sheet, (b) sheet metal with holes, and (c) sheet-metal model with stiffener application. Figure 5 shows that the largest amplitude occurred in the metal-sheet model with a hole, while the sheet-metal model with a stiffener was the model with the lowest amplitude. The amplitudes of the models of the virgin metal sheet, metal sheet with holes, and metal sheet with stiffener were 188, 218, and 73.6 mm, respectively. Each model experienced maximal

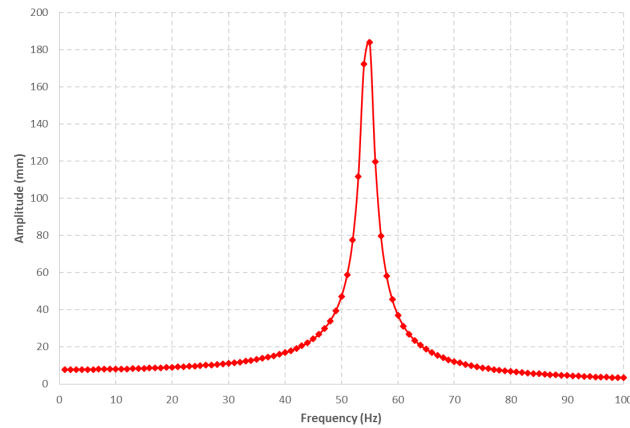
amplitude at different frequencies. For the virgin metal sheet, it occurred at a frequency of 52 Hz; for the metal sheet with holes, it occurred at a frequency of 50.5 Hz; and for the sheet metal with a stiffener, it occurred at a frequency of 82 Hz. Conversely, at the same frequency, amplitude was

different. This shows that the three models had different natural frequencies due to design changes.

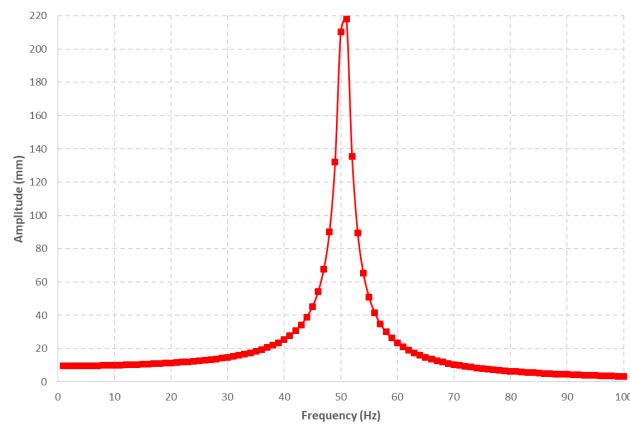
Figure 6 is a picture of the total deformation shown on the basis of its contour with the same classification of material types, namely, marine material or AISI 1090. Figure 6a–c show that each model variation showed signifi-

Table 8: Contours of total deformation from Modes 2 and 12 on different models (low-carbon steel material)

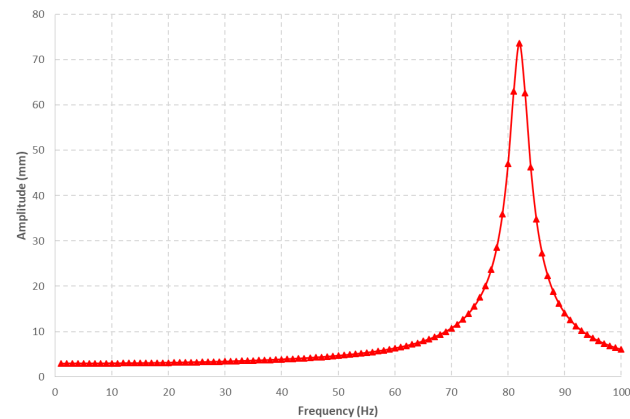
Variant	3	Mode	12
Virgin metal sheet	<div><p>A: Modal Figure Type: Total Deformation Frequency: 333,29 Hz Unit: mm 23/12/2020 0:05</p><p>109,73 Max 97,537 85,345 73,153 60,961 49,769 36,576 24,384 12,192 0 Min</p></div>	<div><p>A: Modal Figure Type: Total Deformation Frequency: 2201,5 Hz Unit: mm 23/12/2020 0:14</p><p>155,59 Max 138,3 121,02 103,73 86,44 69,152 51,864 34,576 17,288 0 Min</p></div>	
Hole metal sheet	<div><p>A: Modal Figure Type: Total Deformation Frequency: 312,71 Hz Unit: mm 23/12/2020 0:07</p><p>106,46 Max 94,635 82,806 70,977 59,147 47,318 35,489 23,660 11,831 0 Min</p></div>	<div><p>A: Modal Figure Type: Total Deformation Frequency: 1751,4 Hz Unit: mm 23/12/2020 0:15</p><p>123,14 Max 109,46 95,779 82,096 68,414 54,731 41,048 27,365 13,682 0 Min</p></div>	
Stiffener metal sheet	<div><p>A: Modal Figure Type: Total Deformation Frequency: 430,23 Hz Unit: mm 23/12/2020 0:04</p><p>118,31 Max 105,17 92,021 78,876 65,73 52,584 39,439 26,294 13,146 0 Min</p></div>	<div><p>A: Modal Figure Type: Total Deformation Frequency: 1732,7 Hz Unit: mm 23/12/2020 0:12</p><p>160,44 Max 142,62 124,79 106,96 89,135 71,308 53,481 35,654 17,827 0 Min</p></div>	



(a)



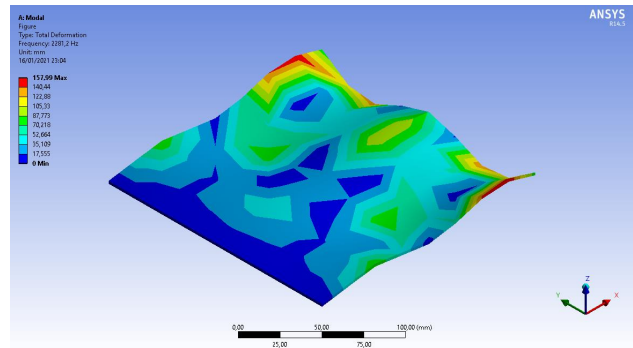
(b)



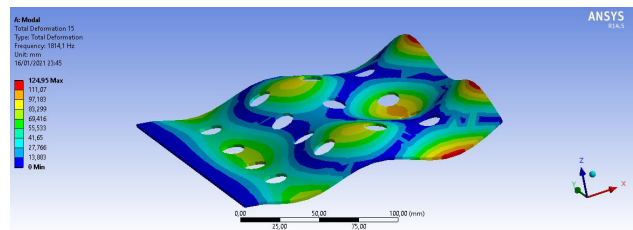
(c)

Figure 5: Frequency vs. amplitude of low-carbon steel materials: (a) virgin metal sheet; (b) hole metal sheet; (c) stiffener metal sheet

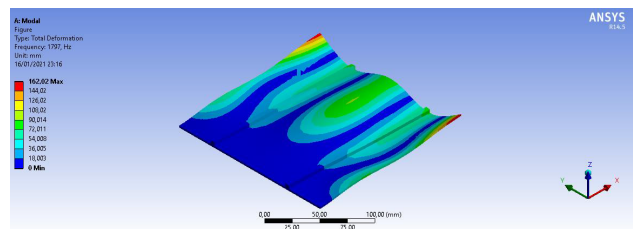
cantly different deformations in the same mode. The taken mode was Mode 12, simulating modal analysis with a random frequency. The deformation that occurred in Figure 6a looked quite even, and the worst deformation in the virgin metal-sheet model or without the addition of holes or



(a)



(b)



(c)

Figure 6: Total deformation contour of marine materials: (a) virgin metal sheet; (b) hole metal sheet; (c) stiffener metal sheet

stiffener occurred at the corners of both sides of the model; deformation in the middle did not look bad. In Figure 6b, the sheet-metal model with holes looks worse than all the other models, with the four worst deformation points in this model. Deformation concentrations occurred in almost every part of this model. This was due to the holes in this model, so that in the section of the path between the two holes, there was a fairly bad concentration of deformation. Figure 6c shows that the sheet-metal model with a stiffener was the best because the worst deformation only occurred on a small scale at the corners of both sides of the model. The center and whole of the model showed better deformation because there were two reinforcements along the sheet-metal model. As a result, the sheet metal became more rigid.

Figure 7 shows the total deformation contours of the same model with different materials. The used material was ice-class material AR 235. Although the results were very

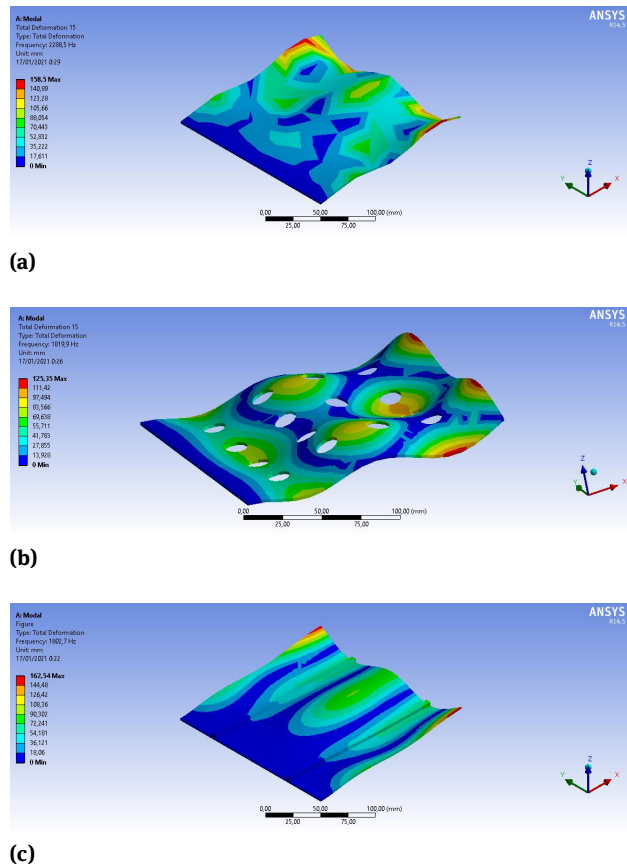


Figure 7: Total deformation contour of ice class materials: (a) virgin metal sheet; (b) hole metal sheet; (c) stiffener metal sheet

significant among the three models, compared to marine materials, the simulation results did not show significant difference.

However, when comparing all the materials that were simulated – low-carbon steel, marine material, and ice-class material in the same mode and variation – the ice-class material had the worst maximal deformation. The maximal deformation that occurred in the 12th mode of the virgin metal sheet model was 158.5, while the maximal deformation that occurred in the low-carbon steel and marine material with the same mode and model was 155.59 and 157.99, respectively. This was because of differences in material properties.

5 Conclusions

Modal-analysis simulation with the resulting random vibration showed that the different designs or models given to each metal sheet changed its characteristics and, especially, its natural frequency. As a result, the performance of the

three models was different. In addition to design models that can change the characteristics of sheet metal, different types of materials also have different characteristics, which is indicated by the different natural frequencies for each material with the same simulation process and model. Good or bad performance depends on the application of the material and model. However, capital analysis using FEA or FEM proved that variation in the model was very significant. In this case, it was evidenced by the first natural mode frequency generated for each different model with the same material; the virgin metal sheet, hole, and stiffener models were 52.50, 50.57, and 82.02 Hz, respectively. Meanwhile, the frequency of the first natural mode in the same model with different materials, low-carbon steel, marine materials, and ice-class materials was 82.02, 84.94, and 85.21 Hz, respectively.

Funding information: This work was supported by the RKAT PTNBH Universitas Sebelas Maret, Surakarta under Scheme of “Penelitian Unggulan UNS” (PU-UNS) – Year 2021, with Grant/Contract No. 260/UN27.22/HK.07.00/2021. The support is gratefully acknowledged by the authors.

Author contributions: All authors have accepted responsibility for the entire content of this manuscript and approved its submission.

Conflict of interest: The authors state no conflict of interest.

References

- [1] Kim T, Lee U. Vibration analysis of thin plate structures subjected to a moving force using frequency-domain spectral element method. *Shock Vib.* 2018;2018:1908508.
- [2] Chan TH, Ashebo DB. Theoretical study of moving force identification on continuous bridges. *J Sound Vibrat.* 2006;295(3-5):870–83.
- [3] Law SS, Bu JQ, Zhu XQ, Chan SL. Moving load identification on a simply supported orthotropic plate. *Int J Mech Sci.* 2007;49(11):1262–75.
- [4] Sniady P. Dynamic response of a Timoshenko beam to a moving force. *J Appl Mech.* 2008;75(2):024503.
- [5] Amiri JV, Nikkhoo A, Davoodi MR, Hassanabadi ME. Vibration analysis of a Mindlin elastic plate under a moving mass excitation by eigenfunction expansion method. *Thin-walled Struct.* 2013;62:53–64.
- [6] Fryba L. Vibration of solids and structures under moving loads. 3rd ed. Groningen: Noordhoff International Publishing; 1999. <https://doi.org/10.1680/vosasumil.35393>.
- [7] Ghafoori E, Kargarnovin MH, Ghahremani AR. Dynamic responses of a rectangular plate under motion of an oscillator using a semi-

- analytical method. *J Vib Control*. 2011;17(9):1310–24.
- [8] Bajer CI, Dyniewicz B. Numerical analysis of vibrations of structures under moving inertial load. Berlin: Springer; 2012. <https://doi.org/10.1007/978-3-642-29548-5>.
 - [9] Shadnam MR, Rofooei FR, Mofid M, Mehri B. Periodicity in the response of nonlinear plate, under moving mass. *Thin-walled Struct*. 2002;40(3):283–95.
 - [10] Yang Y, Ding H, Chen LQ. Dynamic response to a moving load of a Timoshenko beam resting on a nonlinear viscoelastic foundation. *Acta Mech Sin*. 2013;29(5):718–27.
 - [11] Vosoughi AR, Malekzadeh P, Razi H. Response of moderately thick laminated composite plates on elastic foundation subjected to moving load. *Compos Struct*. 2013;97:286–95.
 - [12] Wang X, Jin C. Differential quadrature analysis of moving load problems. *Adv Appl Math Mech*. 2016;8(4):536–55.
 - [13] Esmailzadeh E, Ghorashi M. Vibration analysis of Timoshenko beams subjected to a traveling mass. *J Sound Vibrat*. 1997;199(4):615–28.
 - [14] Gbadeyan JA, Dada MS. Dynamic response of a Mindlin elastic rectangular plate under a distributed moving mass. *Int J Mech Sci*. 2006;48(3):323–40.
 - [15] Wu JS, Lee ML, Lai TS. The dynamic analysis of a flat plate under a moving load by the finite element method. *Int J Numer Methods Eng*. 1987;24(4):743–62.
 - [16] Wu JJ, Whittaker AR, Cartmell MP. The use of finite element techniques for calculating the dynamic response of structures to moving loads. *Comput Struct*. 2000;78(6):789–99.
 - [17] Ghafoori E, Asghari M. Dynamic analysis of laminated composite plates traversed by a moving mass based on a first order theory. *Compos Struct*. 2010;92(8):1865–76.
 - [18] Mohebbpour SR, Malekzadeh P, Ahmadzadeh AA. Dynamic analysis of laminated composite plates subjected to a moving oscillator by FEM. *Compos Struct*. 2011;93(6):1574–83.
 - [19] Baltzis KB. The finite element method magnetics (FEMM) free-ware package: May it serve as an educational tool in teaching electromagnetics? *Educ Inf Technol*. 2010;15(1):19–36.
 - [20] Meeker D. Finite element method magnetics version 4.2 user manual; 2015.
 - [21] Li WH, Du H, Guo NQ. Finite element analysis and simulation evaluation of a magnetorheological valve. *Int J Adv Manuf Technol*. 2003;21(6):438–45.
 - [22] Chen X, Liu Y. Finite element modeling and simulation with ANSYS Workbench. 2nd ed. Florida: CRC Press; 2011.
 - [23] Madenci E, Guven I. The finite element method and applications in engineering using ANSYS. New York: Springer; 2006.
 - [24] Wu J. Free vibration characteristics of a rectangular plate carrying multiple three-degree-of-freedom spring-mass systems using equivalent mass method. *Int J Solids Struct*. 2006;43(3-4):727–46.
 - [25] Ewins D. Modal Testing: Theory and Practice. New York: John Wiley and Sons; 1984.
 - [26] Jrad W, Mohri F, Robin G, Daya EM, Al-Hajjar J. Analytical and finite element solutions of free and forced vibration of unrestrained and braced thin-walled beams. *J Vib Control*. 2020;26(5-6):255–76.
 - [27] Dimitri R, Fantuzzi N, Tornabene F, Zavarise G. Innovative numerical methods based on SFEM and IGA for computing stress concentrations in isotropic plates with discontinuities. *Int J Mech Sci*. 2016;118:166–87.
 - [28] Louhghalam A, Igusa T, Park C, Choi S, Kim K. Analysis of stress concentrations in plates with rectangular openings by a combined conformal mapping – Finite element approach. *Int J Solids Struct*. 2011;48(13):1991–2004.
 - [29] Vanam BC, Rajyalakshmi M, Inala R. Static analysis of an isotropic rectangular plate using finite element analysis (FEA). *J. Mech Eng Res*. 2012;4:148–62.
 - [30] Elsheikh A, Wang D. Large-deflection mathematical analysis of rectangular plates. *J Eng Mech*. 2005;131(8):809–21.
 - [31] Bakker MC, Rosmanit M, Hofmeyer H. Approximate large deflection analysis of simply supported rectangular plates under transverse loading using plate post-buckling solution. *Thin-walled Struct*. 2008;46(11):1224–35.
 - [32] Liew KM, Teo TM, Han JB. Three-dimensional static solutions of rectangular plates by variant differential quadrature method. *Int J Mech Sci*. 2001;43(7):1611–28.
 - [33] Alaimo A, Orlando C, Valvano S. Analytical frequency response solution for composite plates embedding viscoelastic layers. *Aerosp Sci Technol*. 2019;92:429–45.
 - [34] Valvano S, Alaimo A, Orlando C. Sound transmission analysis of viscoelastic composite multilayered shells structures. *Aerospace (Basel)*. 2019;6(6):69.
 - [35] Jain NK. Analysis of stress concentration and deflection in isotropic and orthotropic rectangular plates with central circular hole under transverse static loading. *Int J Mech Mecharon Eng*. 2009;3:1513–9.
 - [36] Chaudhuri RA. Stress concentration around a part through hole weakening laminated plate. *Comput Struct*. 1987;27(5):601–9.
 - [37] Paul TK, Rao KM. Finite element evaluation of stress concentration factor of thick laminated plates under transverse loading. *Comput Struct*. 1989;48(2):311–7.
 - [38] Steen E, Byklum E. Approximate buckling strength analysis of plates with arbitrarily oriented stiffeners. *Proceedings of the 17th Nordic Seminar on Computational Mechanics*; 2004.
 - [39] Troipsky MS. Stiffened plates, bending, stability, and vibration. *J Appl Mech*. 1976;44(3):516.
 - [40] Pape D, Fox AJ. Deflection Solutions for Edge Stiffened Plates. *Proceedings of the 2006 IJME - INTERTECH Conference*; 2006.
 - [41] Xuan HN, Rabczuk T, Alain SP, Dedongnie JF. A smoothed finite element method for plate analysis. *Comput Methods Appl Mech Eng*. 2008;197(13-16):1184–203.
 - [42] Das D, Prasanth S, Saha K. A variational analysis for large deflection of skew plates under uniformly distributed load through domain mapping technique. *Int J Eng Sci Technol*. 2009;1:16–32.
 - [43] Alaimo A, Orlando C, Valvano S. An alternative approach for modal analysis of stiffened thin-walled structures with advanced plate elements. *Eur J Mech A, Solids*. 2019;77:103820.
 - [44] Valvano S, Alaimo A, Orlando C. Analytical analysis of sound transmission in passive damped multilayered shells. *Compos Struct*. 2020;253:112742.
 - [45] Moshaiov MA, Vorus WS. Elasto-plastic plate bending analysis by a boundary element method with initial plastic moments. *Int J Solids Struct*. 1986;22(11):1213–29.
 - [46] Paiva JB, Aliabadi MH. Bending moments at interfaces of thin zoned plates with discrete thickness by the boundary element method. *Eng Anal Bound Elem*. 2004;28(7):747–51.
 - [47] Ramkrishna D, Kumar KK, Krishna Y. Modal testing of beams using Translation-AngularPiezo-beam (TAP) accelerometer. *Adv Vib Eng*. 2008;7:7–14.

- [48] Hu S, Chen W, Gou XF. Modal analysis of fractional derivation damping model of frequency-dependent viscoelastic soft matter. *Adv Vib Eng.* 2011;10:187–96.
- [49] Liu F, Fan R. Experimental Modal Analysis and Random Vibration Simulation of Printed Circuit Board Assembly. *Adv Vib Eng.* 2013;15:489–98.
- [50] Fei WH, Kun-kun J, Zi-peng G. Random vibration analysis for the chassis frame of hydraulic truck based on ANSYS. *J Chem Pharm.* 2014;6:849–52.
- [51] De Boni LA, Lima da Silva IN. Monitoring the transesterification reaction with laser spectroscopy. *Fuel Process Technol.* 2011;92(5):1001–6.
- [52] Turner WM, Clough RW, Martin RW, Topp L. Stiffness and deflection analysis of complex structures. *J Aeronaut Sci.* 1956;25(9):805–23.
- [53] Timoshenko WS, Goodier JN. *Theory of elasticity.* 3rd ed. New York: McGraw-Hill; 1970.
- [54] Song O. *Modal analysis of a cantilever plate.* New Jersey: New Jersey Institute of Technology; 1986.
- [55] Bahiuddin I, Mazlan SA, Shapii I, Imaduddin F, Ubaidillah, Choi SB. Ubaidillah, Choi SB. Constitutive models of magnetorheological fluids having temperature-dependent prediction parameter. *Smart Mater Struct.* 2018;27(9):095001.
- [56] Suyitno ZA, Ahmad AS, Argatya TS. Ubaidillah. Optimization parameters and synthesis of fluorine doped tin oxide for dye-sensitized solar cells. *Appl Mech Mater.* 2014;575:689–95.
- [57] Ridwan R, Prabowo AR, Muhayat N, Putranto T, Sohn JM. Tensile analysis and assessment of carbon and alloy steels using FE approach as an idealization of material fractures under collision and grounding. *Curved Layer Struct.* 2020;7(1):188–98.
- [58] Prabowo AR, Laksono FB, Sohn JM. Investigation of structural performance subjected to impact loading using finite element approach: case of ship-container collision. *Curved Layer Struct.* 2020;7(1):17–28.
- [59] Shabdin MK, Rahman MA, Mazlan SA. Ubaidillah, Hapipi NM, Adiputra D, Aziz SAA, Bahiuddin I, Choi SB. Material characterizations of gr-based magnetorheological elastomer for possible sensor applications: Rheological and resistivity properties. *Materials (Basel).* 2019;12(3):391.
- [60] Courant R. Variational methods for the solution of problems of equilibrium and vibration. *Bull New Ser Am Math Soc.* 1943;49(1):1–23.
- [61] Prabowo AR, Sohn JM. Nonlinear dynamic behaviors of outer shell and upper deck structures subjected to impact loading in maritime environment. *Curved Layer Struct.* 2019;6(1):146–60.
- [62] Clough RW. The finite element method in plane stress analysis. *Proceedings of the 2nd ASCE Conference on Electronic Computation;* 1960.
- [63] Zienkiewicz OC, Cheung YK. *The finite element method in structural and continuum mechanics. Volume 1.* New York: McGraw-Hill. New York; 1967.
- [64] Prabowo AR, Sohn JM, Putranto T. Crashworthiness performance of stiffened bottom tank structure subjected to impact loading conditions: Ship-rock interaction. *Curved Layer Struct.* 2019;6(1):245–58.
- [65] Clough RW. Original formulation of the finite element method. *ASCE Structures Congress Session on Computer Utilization in Structural Engineering;* 1989.
- [66] Argyris J, Tenek L. Recent advances in computational thermostructural analysis of composite plates and shells with strong nonlinearities. *Appl Mech Rev.* 1997;50(5):285–306.
- [67] Prabowo AR, Cao B, Sohn JM, Bae DM. Crashworthiness assessment of thin-walled double bottom tanker: Influences of seabed to structural damage and damage-energy formulae for grounding damage calculations. *J Ocean Eng Sci.* 2020;5(4):387–400.
- [68] Tatsumi A, Fujikubo M. Ultimate strength of container ships subjected to combined hogging moment and bottom local loads part 1: Nonlinear finite element analysis. *Mar Structures.* 2020;69:102683.
- [69] Prabowo AR, Do QT, Cao B, Bae DM. Land and marine-based structures subjected to explosion loading: A review on critical transportation and infrastructure. *Procedia Struct Integr.* 2020;27:77–84.
- [70] Pasaoglu Bozkurt A. Effects of mechanical vibration on miniscrew implants and bone: fem analysis. *Int Orthod.* 2019 Mar;17(1):38–44.